Progressive Alopecia Reveals Decreasing Stem Cell Activation Probability during Aging of Mice with Epidermal Deletion of DNA Methyltransferase 1

Ji Li[1,2], Ting-Xin Jiang[1], Michael W. Hughes[1], Ping Wu[1], Randall B. Widelitz[1], Guoping Fan[3] and Cheng-Ming Chuong[1]

To examine the roles of epigenetic modulation on hair follicle regeneration, we generated mice with a K14-Cre-mediated loss of DNA methyltransferase 1 (DNMT1). The mutant shows an uneven epidermal thickness and alterations in hair follicle size. When formed, hair follicle architecture and differentiation appear normal. Hair subtypes exist but hair fibers are shorter and thinner. Hair numbers appear normal at birth but gradually decrease to <50% of control in 1-year-old mice. Sections of old mutant skin show follicles in prolonged telogen with hyperplastic sebaceous glands. Anagen follicles in mutants exhibit decreased proliferation and increased apoptosis in matrix transient-amplifying cells. Although K15-positive stem cells in the mutant bulge are comparable in number to the control, their ability to proliferate and become activated to form a hair germ is reduced. As mice age, residual DNMT activity declines further, and the probability of successful anagen reentry decreases, leading to progressive alopecia. Paradoxically, there is increased proliferation in the epidermis, which also shows aberrant differentiation. These results highlight the importance of DNA methylation in maintaining stem cell homeostasis during the development and regeneration of ectodermal organs.

Journal of Investigative Dermatology advance online publication, 5 July 2012; doi:10.1038/jid.2012.206

INTRODUCTION

The hair follicle, an organ with robust regenerative capabilities, undergoes episodic regenerative cycling in adults under normal physiological conditions. In adult animals, hair follicles cycle through phases of growth (anagen), regression (catagen), and quiescence (telogen) (Stenn and Paus, 2001; Schmidt-Ullrich and Paus, 2005; Cotsarelis, 2006). The architectural organization of hair follicles makes it easy to discern the location of hair stem cells, proliferating transient-amplifying (TA) cells, and differentiating cells. The length of a hair shaft is proportional to the duration of anagen. Furthermore, >30,000 hair follicles grow on each individual, rendering them accessible to quantitative analyses (Plikus and Chuong, 2008a; Plikus *et al.*, 2011). These characteristics make the hair an ideal model to study homeostasis among stem/TA/differentiated cells within the hair follicle (Blanpain and Fuchs, 2009).

Recently, epigenetic mechanisms involving modifications of histone tails or DNA have been shown to modulate the accessibility of genes to transcriptional machinery and thereby modulate gene activities without having to change the DNA genomic sequence (Goldberg *et al.*, 2007). We wondered what roles epigenetic processes may play in the development and regeneration of hair follicles.

DNA methyltransferase 1 (DNMT1) function has been studied extensively. In the skin, DNA methylation has a role in stem cell self-renewal and differentiation (Sen *et al.*, 2010). These authors showed that DNMT1 is required to maintain epidermal lineage precursor cells. Upon differentiation, the promoters of a number of genes involved in epithelial differentiation were demethylated. The small hairpin RNA-mediated suppression of DNMT1 reduced the progenitor pool as the cells differentiated prematurely.

However, the role of DNMT1 has not been studied in the regenerative cycling of hair follicles, nor in epidermal homeostasis *in vivo*. To assess the roles of DNMT1 in regulating hair filaments and hair follicles during the murine hair cycle, we crossed a K14-Cre line that expresses Cre recombinase in epidermal basal cells with a floxed DNMT1 line to excise specific exons of the *DNMT1* gene in the mouse epidermis. This cross created a conditional knockout of DNMT1 in the K14-expressing epidermis. Here we report the

[1]*Department of Pathology, Keck School of Medicine, University of Southern California, Los Angeles, California, USA;* [2]*Department of Dermatology, Xiang Ya Hospital, Central South University, Changsha, Hunan, China and* [3]*Department of Human Genetics, University of California, Los Angeles, Los Angeles, California, USA*

Correspondence: Cheng-Ming Chuong, Department of Pathology, Keck School of Medicine, University of Southern California, HMR 313B, 2011 Zonal Avenue, Los Angeles, California 90033, USA.
E-mail: cmchuong@usc.edu

Abbreviations: AP, intracisternal A particle; CldU, chlorodeoxyuridine; DNMT1, DNA methyltransferase 1; IdU, iododeoxyuridine; IHC, immunohistochemistry; ORS, outer root sheath; TA cell, transient-amplifying cell; WT, wild type

Received 8 June 2011; revised 10 February 2012; accepted 26 February 2012

skin pathology of these mice and the abnormal stem cell activity in the epidermis and hairs.

RESULTS

DNMT1 is expressed in the developing skin and cycling hair follicles

Hair placodes begin to form at embryonic day 14.5 (E14.5). DNMT1 is expressed widely in the epithelium at this stage. By E16–E18, the epidermis expands to become multilayered and hair germs and hair pegs form. At these stages, DNMT1 is enriched in the basal epidermal layer and hair germs/pegs, but gradually disappears from the spinous, granular, and stratum corneum layers (Figure 1a). After birth, at postnatal days 0–9 (P0–P9), DNMT1 is weakly expressed in the epidermal basal layer and more strongly in the hair matrix (Figure 1a). In adult anagen hair follicles, DNMT1 is expressed in the outer root sheath (ORS), inner root sheath, and matrix, whereas in telogen hair follicles it is mostly expressed in the hair germ (Figure 1b). A schematic summary of DNMT expression is shown (Figure 1c).

Generation and characterization of K14-Cre DNMT1$^{fl/fl}$ mice

To investigate the role of DNMT1 in hair development and cycling, we generated K14-Cre DNMT1$^{fl/fl}$ mice by crossing K14-Cre mice with DNMT1$^{fl/fl}$ mice (Figure 2a). The genotype of all offspring demonstrates the presence of the *LoxP* element and K14-Cre (Figure 2b). Cre-mediated recombination is detected in the dissected epidermis containing hair follicles from K14-Cre DNMT1$^{fl/fl}$ mice. Muscle serves as a negative control. Using primers P1 and P2 to amplify the floxed allele or P1 and P3 to amplify the recombined allele after excision, we find a K14-Cre-mediated specific deletion of DNMT1 in skin epidermis but not in the muscle (Figure 2c). Many but not all genotypic DNMT1-floxed mice show obvious phenotypes. However, there is a good correlation between the level of DNMT1 deletion by recombination and the level of the observed phenotype.

To further characterize DNMT1 loss in the skin of K14-Cre DNMT1$^{fl/fl}$ mice, we performed western blot analysis using anti-DNMT1 antibodies targeted downstream to the excision site. Mice with clear phenotypes show no detectable DNMT1 protein (Figure 2d, right panel), whereas mice without obvious phenotypes show some DNMT1 expression, although less than wild type (WT; Figure 2d, left and middle panels). The DNMT1 deletion is further demonstrated by immunohistochemistry (IHC), which shows a reduction, but not a complete loss, of DNMT1 expression (Figure 2e, right panel).

We also assessed the activity of DNA methylation by measuring levels of intracisternal A particle (IAP). IAP is normally highly methylated and its expression is silenced. However, IAP expression can be reactivated upon DNA hypomethylation (Hutnick *et al.*, 2010). We reasoned that if DNMT1 is effectively deleted in the epidermis, IAP might become expressed to detectable levels. Indeed, immunofluorescence shows that IAP is absent in WT skin but is highly expressed in the ORS, with lower expression in the hair matrix of the mutant (Figure 2e, left panel). Hair matrix cells are supposed to be derived from the ORS. The observation that matrix cells express IAP may be because of changes in methylation activity in the matrix or, by speculation, the expansion of epithelial cells whose DNMT is not completely inactivated. If DNMT is suppressed, we expect that the methylation level by 5-methyl cytosine should also be reduced. IHC showed that there were fewer 5-methyl cytosine–positive cells (Figure 2e, middle panel).

Gross phenotypes in DNMT1-deleted mice

At P3, no major phenotype differences are observed (not shown). At P7 and P9, K14-Cre DNMT1$^{fl/fl}$ mice are smaller and exhibit slight delays in hair development. By 2 months, K14-Cre DNMT1$^{fl/fl}$ mice start to show alopecia phenotypes. Body hairs are sparse and short compared with controls. Hairless patches also appear on the trunk. By 1 year, the K14-Cre DNMT1$^{fl/fl}$ mice have grown to equal the size of controls but still exhibit a sparse and ruffled hair coat (Figure 3a and a′). For further quantification, dorsal skin was excised, inverted, and hair density was measured under a dissection microscope (Figure 4). At 2 months of age, no significant difference in hair density is observed (Figure 3b and b′; WT: 59.6 ± 0.9 hairs mm^{-2}, K14-Cre DNMT1$^{fl/fl}$ 60.4 ± 1.2 hairs mm^{-2}, $P > 0.05$). At 1 year, hair density is less than half of that found in normal littermates (Figure 3b and b′. WT: 53.2 ± 1.0 hairs mm^{-2}, K14-Cre DNMT1$^{fl/fl}$ 25.6 ± 3.0 hairs mm^{-2}, $P < 0.05$).

K14-Cre DNMT1$^{fl/fl}$ mouse vibrissae are curly and short (not shown). Their pelage consists of four hair types: guard, awl, auchene, and zigzag, each with a distinctive morphology (Figure 3c). We wondered whether certain hair types develop abnormally or are lost preferentially because of reduced DNA methylation. Examination shows that the ratio of different hair types is similar. However, we observe a reduction of hair size in both diameter and length. This is seen in all hair types (Figure 3d, $P < 0.05$). Secondary hairs from K14-Cre DNMT1$^{fl/fl}$ have a reduced diameter and appear to be only half the length of WT. In general, the K14-Cre DNMT1$^{fl/fl}$ mouse hairs are thinner than the corresponding wild-type hairs. In many of the awl hairs, the normal 3 to 4 columns of medulla cells are reduced to 1 to 2 columns (Figure 3d, lower panel).

Histopathology and molecular characterization of DNMT1-deleted skin

DNMT1-deleted skin exhibits unevenness in the thickness of the skin and follicle size of hairs. Some hair follicles have a wider hair canal (Figure 4b and d). However, the general architecture of hair follicles and filaments, which do form, show no obvious abnormalities.

We used IHC to explore whether abnormal hair differentiation occurred in the skin of adult K14-Cre DNMT1$^{fl/fl}$ mice (Figure 4a and b). As in controls, K10 is expressed in the differentiated skin keratinocytes. However, in contrast to control skin, involucrin IHC showed precocious expression in some basal layer cells and patchy staining in suprabasal cells of the mutant.

In telogen follicles, p63 is present in the basal epithelium of follicular and interfollicular skin. K15 is present in the hair germ of telogen follicles. K14 antibody stains the basal layer of the skin and ORS layer of the follicle (Figure 4d). CD34 IHC staining does not show differences between mutant and wild-type hair follicles (not shown). On the other hand, P16, a cell cycle suppressor, is increased in the ORS of mutant

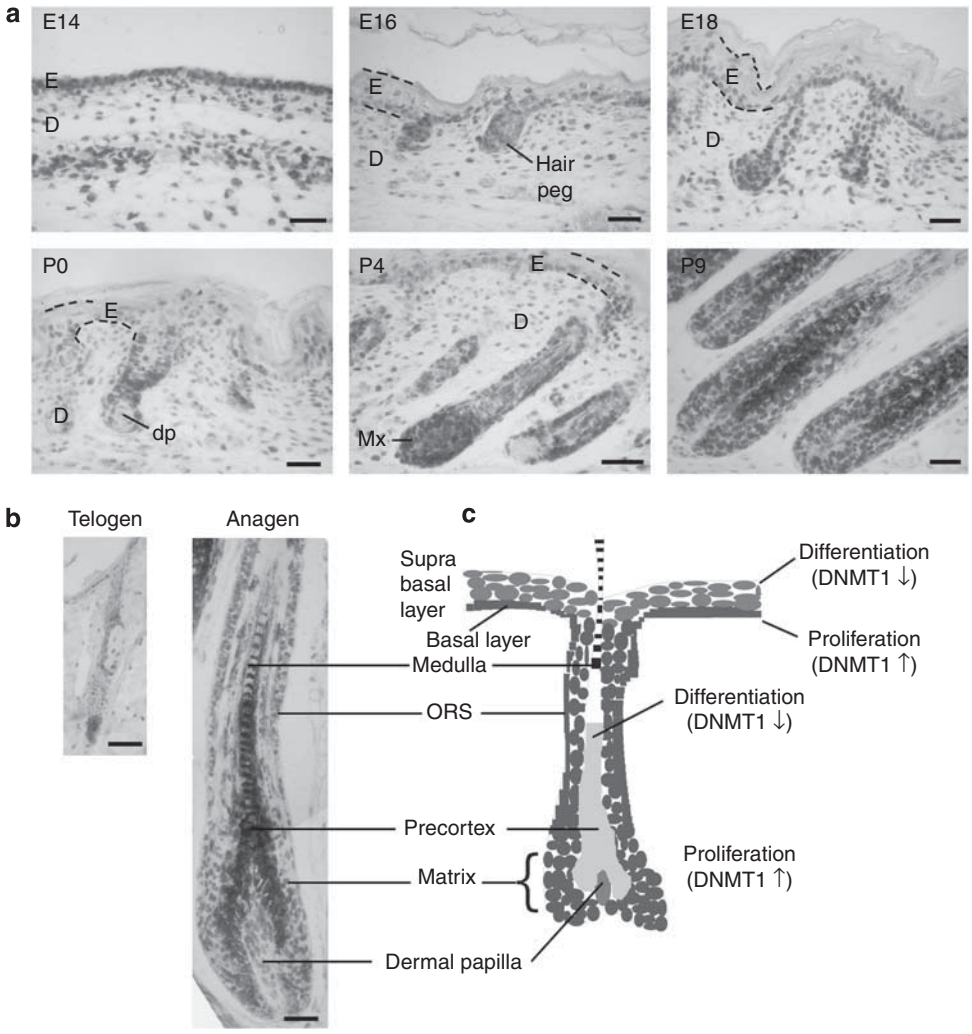

Figure 1. Expression of DNA methyltransferase 1 (DNMT1) in developing and cycling hair follicles. (**a**) Sections of mouse dorsal skin at embryonic days 14 and 16 (E14 and E16), and postnatal days 0, 4, and 9 (P0, P4, and P9) were subjected to immunohistochemistry. DNMT1 is mainly expressed in the basal layer of the epithelium and hair matrix. Some DNMT1 was seen in the dermis. (**b**) In the adult, DNMT1 was expressed in the outer root sheath (ORS) and matrix region of anagen follicles, and in hair germ region in telogen. (**c**) Schematic highlighting the expression. DNMT1 is low in the differentiating suprabasal layer and hair shaft. D, dermis; dp, dermal papilla; E, epidermis; Mx, matrix. Bar = 50 μm.

follicles. CD200, which is expressed in the hair germ in the bulge area, is decreased in mutant hair follicles.

In anagen follicles, the mAb AE15 stains the inner root sheath and medulla of the hair shaft. AE13 stains the precortex and the cortex of the hair shaft (Lynch *et al.*, 1986). There are no distinct differences in expression patterns of hair differentiation markers between WT and mutant mice.

Progressive changes during aging of DNMT1-deleted mouse skin

We wondered whether this loss of hair fibers reflects a comparable loss of hair follicles in the skin of K14-Cre DNMT1$^{fl/fl}$ mice. The hematoxylin and eosin–stained sections of 1-year-old mouse skin show that hair follicle density is reduced, only by ~25%, in K14-Cre DNMT1$^{fl/fl}$ mice compared with their control littermates (Figure 4c and d). Another marked difference is that mutant skin shows a large percentage of telogen follicles, whereas the WT skin contains patches of anagen and telogen hairs (Figure 4d).

We tried to observe the progression of a regenerative hair wave (Plikus and Chuong, 2008a; Plikus *et al.*, 2008b, 2011). In the mutant, the skin remains static and many follicles fail to reenter anagen even after 80 days (not shown). Telogen duration is longer in the mutant than in the WT, whereas the length of anagen is similar between mutant and WT hair cycles (Figure 4e). Many telogen follicles in mutant skin are empty without club hairs and are surrounded by hyperplastic sebaceous glands (Figure 4d). These results suggest that either the prolonged telogen enables follicles to lose their club hairs or that there are defects in retaining club hairs.

DNMT1-deleted mice show reduced proliferation in anagen hair matrix

In anagen, TA cells in the matrix proliferate and then move upward and differentiate into the hair shaft (Zhang *et al.*, 2009). We analyzed the dynamics of cell proliferation. First,

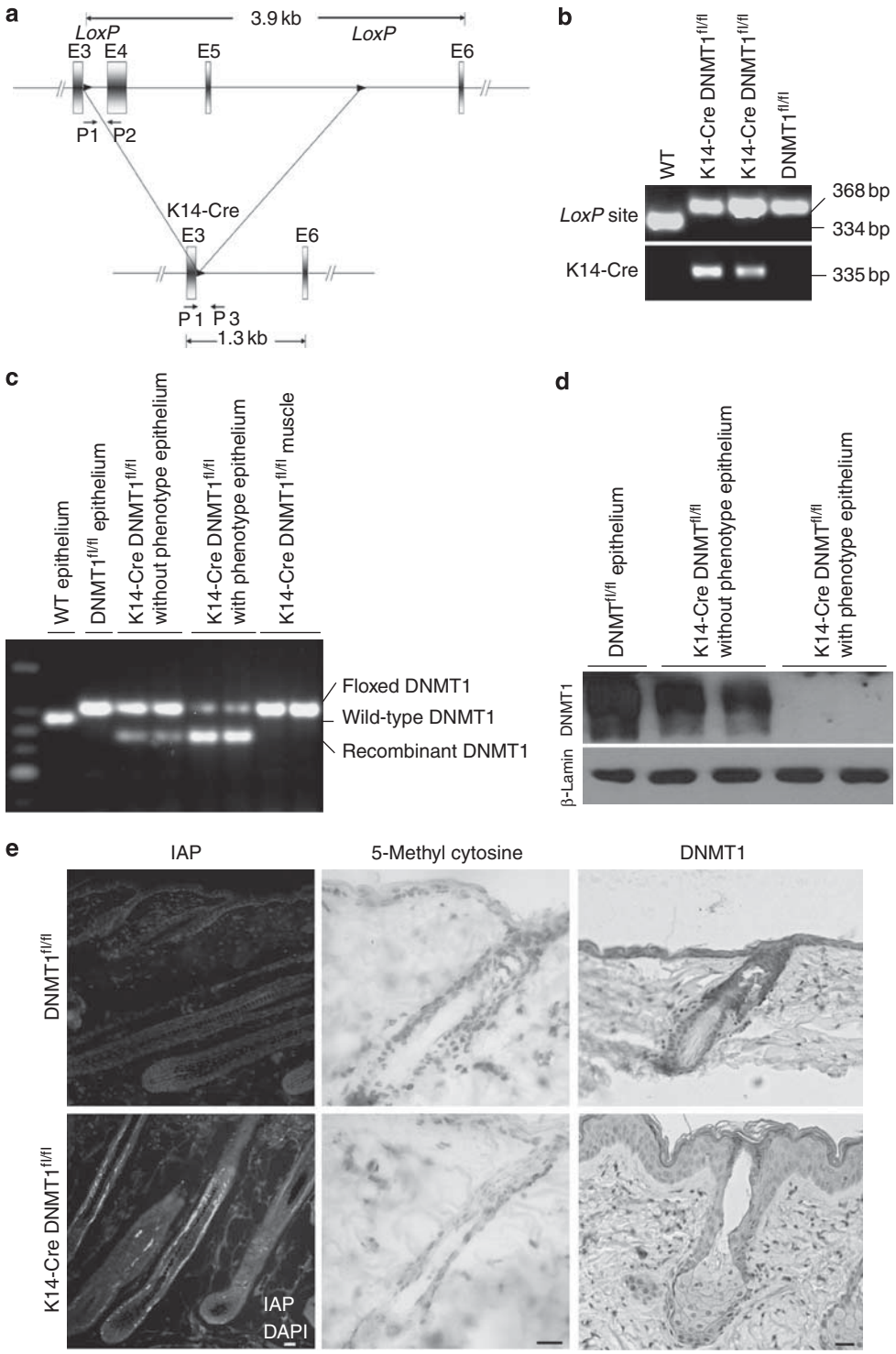

Figure 2. Genotyping and conditional deletion efficiency of K14-Cre DNMT1$^{fl/fl}$ mice. (**a**) K14-Cre DNMT1$^{fl/fl}$ DNA schematic (Jackson-Grusby *et al.*, 2001). (**b**) PCR amplification of *LoxP* and Cre. (**c**) PCR amplification of floxed versus Cre-mediated excision of DNA methyltransferase 1 (DNMT1). High DNMT1 excision levels are associated with a phenotype. Muscle is a negative control. (**d**) Western blot quantification of DNMT1. DNMT1 protein levels inversely correlated with a phenotype. (**e**) Intracisternal A particle (IAP), 5-methyl cytosine, and DNMT1 expression were detected by immunohistochemistry (IHC). IAP level was elevated, whereas 5-methyl cytosine and DNMT1 levels were decreased in mutant mice compared with wild type (WT). Bar = 10 μm. DAPI, 4,6-diamidino-2-phenylindole.

BrdU was used to label proliferating cells. Three-month-old mice at day 6 in anagen were labeled with BrdU for 1 hour. We can see that there are fewer labeled cells in the mutant's matrix, ORS, and bulge area (Figure 5a). The number of BrdU-positive cells in the hair matrix, ORS, and bulge area was quantified (WT = 52.17 ± 5.42, 6.31 ± 3.22, and 1.83 ± 1.17, respectively; K14-Cre DNMT1$^{fl/fl}$ = 22 ± 3.03, 4.38 ± 2.13, and 1 ± 0.89, respectively). We also calculated the mitotic index and

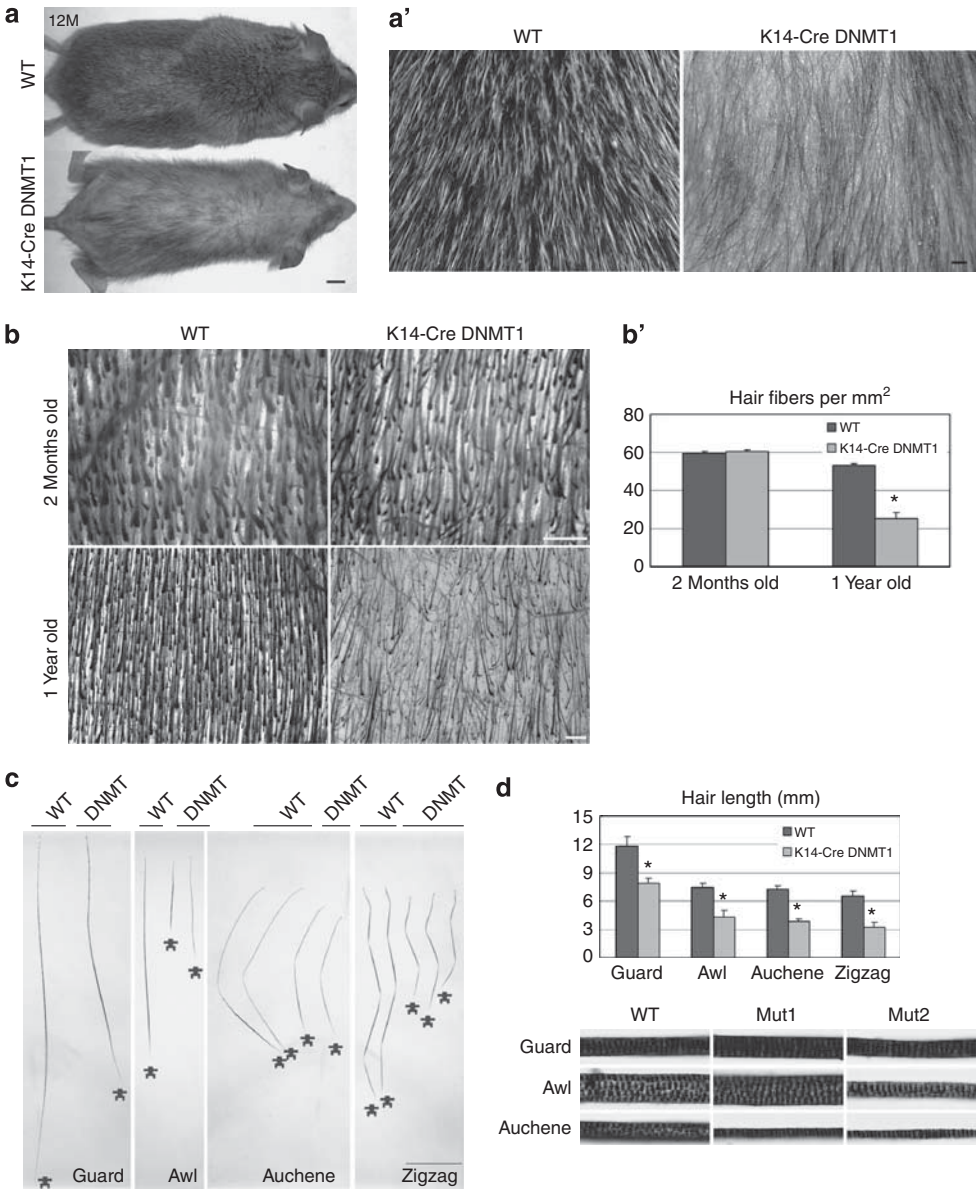

Figure 3. K14-Cre DNMT1$^{fl/fl}$ mice show reduced hair size in all hair types, and reduction of hair density in older mice. (**a**) One-year-old control and mutant. Bar = 0.5 cm. (**a'**) Enlargement. Mutant hair is thinner in size and reduced in number. Bar = 1 mm. (**b**) Hair numbers gradually decrease from 2 months to 1 year. Bar = 50 μm. (**b'**) Density of hair fibers in mutant and wild-type (WT) mice in young and old mice. Shown as mean ± SD. (**c**) Comparison of guard, awl, auchene, and zigzag hairs. Shapes are generally fine, but mutant hairs are shorter. Bar = 3 mm. (**d**) Both hair length and width are reduced. Medulla and width of different hair types. Mutant 2 is more affected than mutant 1. Bar = 0.2 mm. (**d**, bottom) Quantitative comparison of hair lengths by types (mean ± SD). DNMT1, DNA methyltransferase 1.

found that there was a reduction of BrdU-positive cells/total cell number from 58 to 40% (Figure 5a'; $P<0.05$).

Thereafter, we estimated the upward movement of TA cells in the hair matrix using double labeling with chlorodeoxyuridine (CldU) and iododeoxyuridine (IdU), followed by a chase period. In the hair follicle, most cell proliferation occurs in the matrix below Auber's line, which traverses the largest diameter of the dermal papilla (Peters *et al.*, 2002). We expect that cells labeled earlier should move more toward the distal bulb, whereas newly labeled cells should be close to the base, or beneath Auber's line.

We labeled mice with CldU for 11.5 hours followed by a short IdU labeling period of 0.5 hours. At the end of the 0.5-hour period, mice are killed and the distribution of both CldU (red)- and IdU (green)-positive cells are examined. In the WT follicles, we observe many CldU-positive cells and roughly half are above Auber's line. In mutant follicles, there are fewer CldU-positive cells, consistent with the decrease of cell proliferation (Figure 5a). Furthermore, only approximately one-third of CldU-labeled cells are above Auber's line, implying a reduced rate of upward movement (Figure 5b and b', red color). IdU-positive cells have entered S phase within the most recent 0.5 hours. Most of them lay beneath Auber's

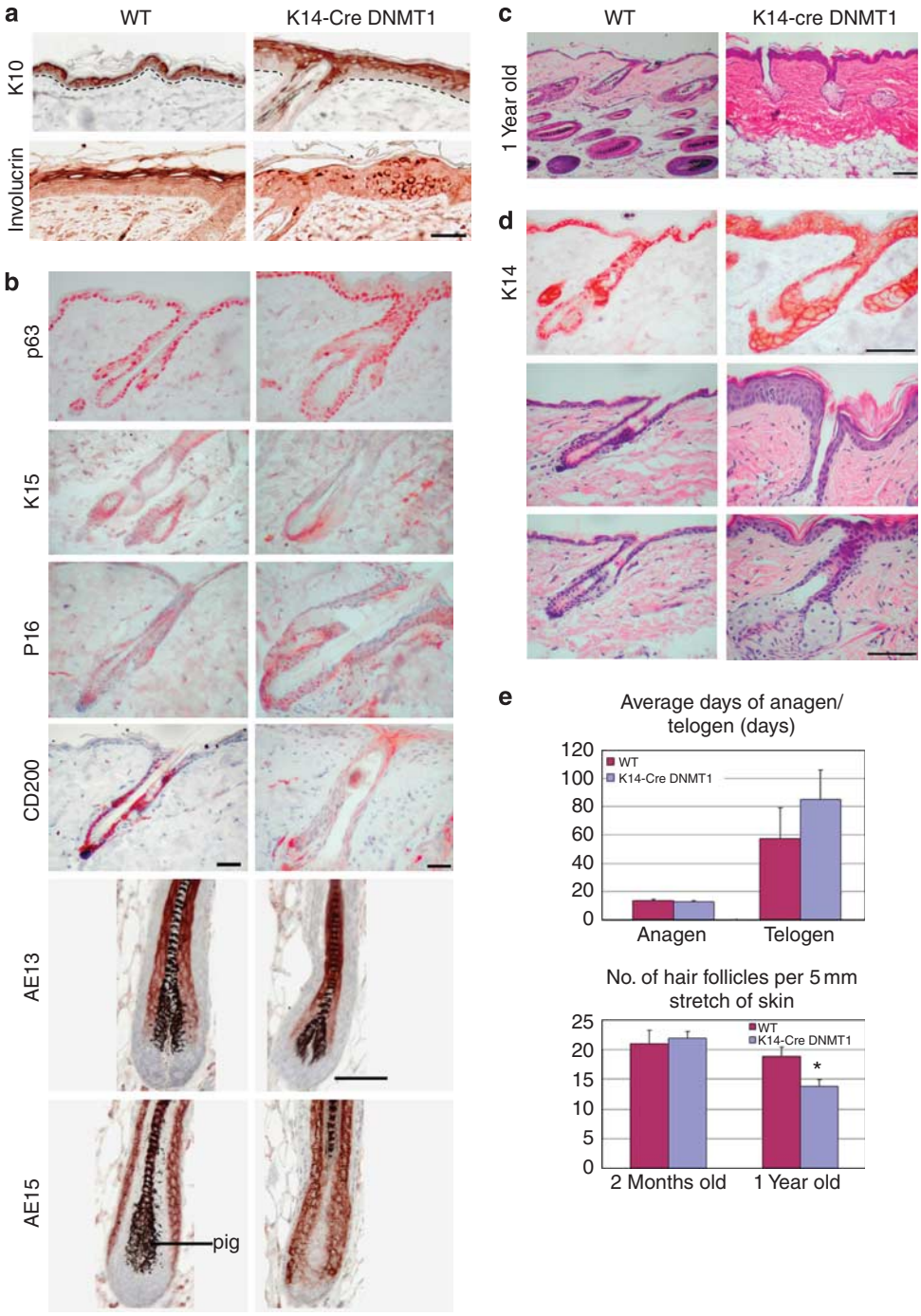

Figure 4. Molecular characterization of K14-Cre DNMT1$^{fl/fl}$ mouse skin. (**a**) Mutant shows unevenness in the thickness of the epidermis and the size of hair follicles. Some follicles show larger diameter follicles and hair canals, but others are smaller. Otherwise, the morphology of hair follicles appears normal. Immunohistochemistry (IHC) of 3-month-old mutants shows wide and patchy expression of involucrin. (**b**) IHC shows that mutants have normal expression of p63, K15, AE13, and AE15, but reduced CD200 and increased P16 expression. Bar = 50 μm. (**c**) One-year-old mutant skin is mainly composed of telogen follicles. (**d**, first row) Skin from old mutants shows most follicles in telogen, and many without club hairs. K14 IHC appears normal. (**d**, second row) Uneven thickness of epidermis is obvious. (**d**, third row) Enlarged sebaceous glands. Bar = 0.4 mm. (**e**) Anagen duration is about the same in 1-year-old mutants, but telogen duration increases significantly. Old mutants showed decreased hair follicle density. Bar diagram is shown as mean ± SD. Two-tailed unpaired Student's *t*-tests were used (*$P<0.05$). DNMT1, DNA methyltransferase 1; WT, wild type.

line (Figure 5b and b′, green color). Thus, TA cells in WT follicles proliferate and progress to hair filament differentiation, extending much further into the distal follicle than TA cells in K14-Cre DNMT1$^{fl/fl}$ hair follicles.

DNMT1-deleted mice show decreased numbers of label-retaining cells in the stem cell region

To gauge the ability of DNMT1 to maintain progenitor stem cells, we measured the population size of long-term label-

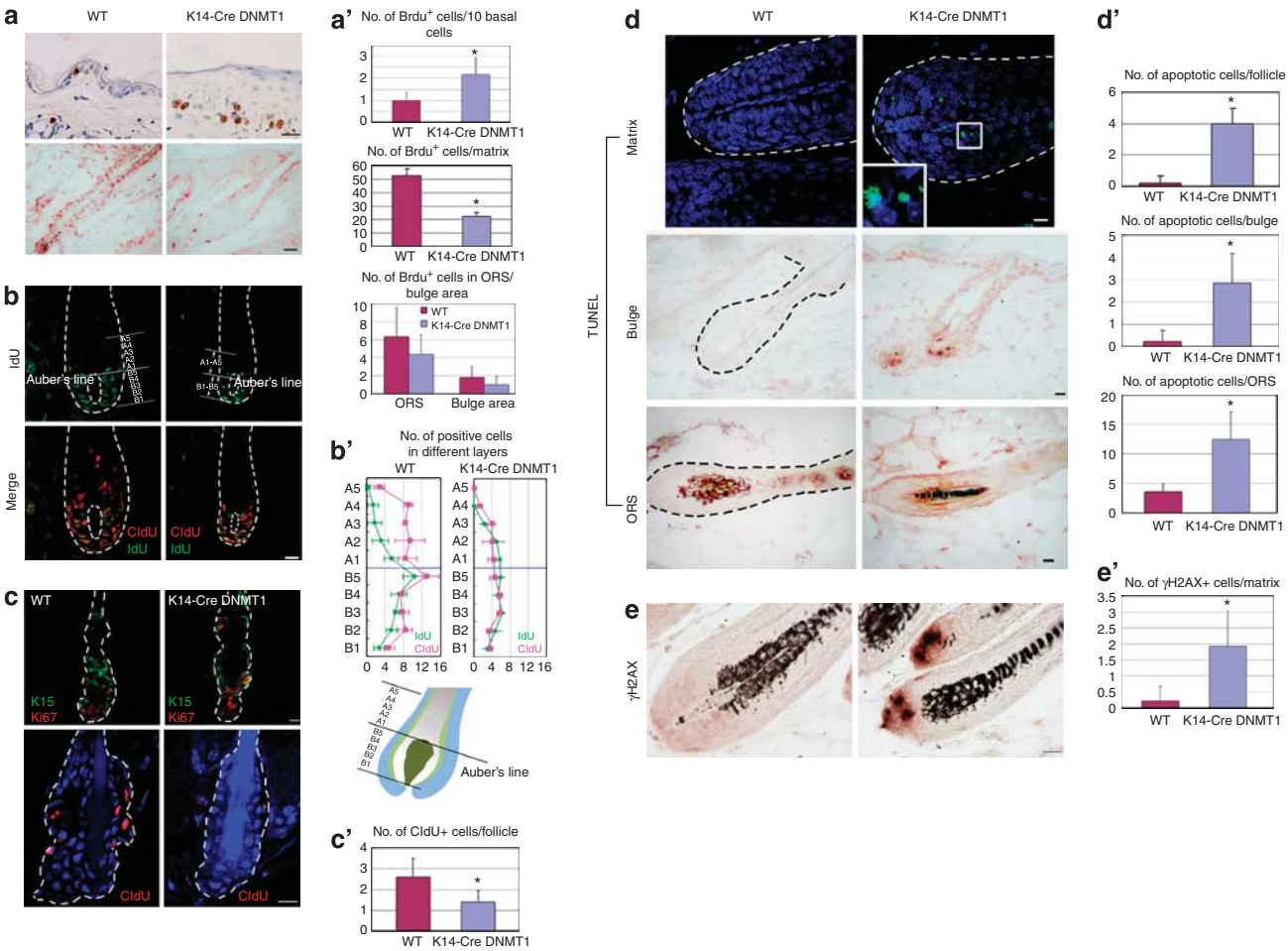

Figure 5. K14-Cre DNMT1$^{fl/fl}$ hair follicles show reduced proliferation and increased apoptosis in hair follicles. (**a**) One-hour BrdU labeling of 3-month-old mice. In the epidermis, BrdU labeling is increased, but reduced in the hair matrix and outer root sheath (ORS). Bar = 20 μm. (**a′**) Numbers were quantified (**a′**, mean ± SD). (**b**) Cells were labeled with chlorodeoxyuridine (CldU; red) for 11.5 hours, followed by iododeoxyuridine (IdU; green) for 30 minutes. CldU cells moved above Auber's line in wild type (WT), but not in mutant cells. Bar = 50 μm. (**b′**, upper) Numbers of CldU- or IdU-positive cells along the proximal–distal axis of hair follicle were quantified. (**c**) Double staining with K15 (green) and Ki67 (red) in telogen follicles and long-term label retention of CldU. The label-retaining cell (LRC) number was lower in mutants. Bar = 10 μm. (**c′**) Quantification. Student's *t*-test (*$P<0.05$). (**d**) TUNEL-positive cells (green fluorescent or brown immunohistochemistry (IHC)) in the matrix, bulge, and ORS of mutants. The 4,6-diamidino-2-phenylindole (DAPI) stains nucleus (blue). (**d′**) Average number of TUNEL-positive cells per follicle, bulge, or ORS (mean ± SD). (**e**) γH2AX, indicator of DNA damage, is increased in hair bulbs (brown in IHC). (**e′**) Numbers of γH_2AX-positive cells in follicle matrix were quantified (mean ± SD). Bar = 20 μm.

retaining cells. We injected CldU into newborn pups from postnatal days 3–5 followed by an 8 week change period ($n=3$). Long-term label-retaining cells were analyzed by CldU staining (Figure 5c, lower). The number of CldU-positive cells per follicle was lower in the mutant than in the WT (three follicles per mouse; Figure 5c′; $P<0.05$). We stained follicles in very early anagen with K15 and Ki67 antibodies (Figure 5c, upper). It appears that hair stem cells in the K14-Cre DNMT1$^{fl/fl}$ mice can be activated properly during early anagen.

DNMT1-deleted mice show increased apoptosis in anagen hair follicles

We examined levels of apoptosis using the TUNEL assay. There are significantly more TUNEL-positive cells in the matrix, ORS, and bulge area of the K14-Cre DNMT1$^{fl/fl}$ mice (Figure 5d and d′. $P<0.05$). As DNMT1 has been shown to participate in DNA repair processes (Mortusewicz *et al.*, 2005), we also examined the expression of γH2AX, a marker for DNA damage. We observed many more γH_2AX-positive cells in K14-Cre DNMT1$^{fl/fl}$ mice compared with WT (Figure 5e and e′, $P<0.05$).

Delayed activation of hair stem cells after hair plucking in K14-Cre DNMT1$^{fl/fl}$ mice

We wondered whether hair stem cells could respond to activation signals properly. We used wax stripping to test the response. A 1-cm^2 region of dorsal skin is stripped of hairs. By 11 days after plucking, hairs have regenerated in controls but not in the K14-Cre DNMT1$^{fl/fl}$ mice (Figure 6a, middle panel). The regeneration of hairs from mutant stem cells is significantly delayed but occurs at day 21 (Figure 6a, right panel).

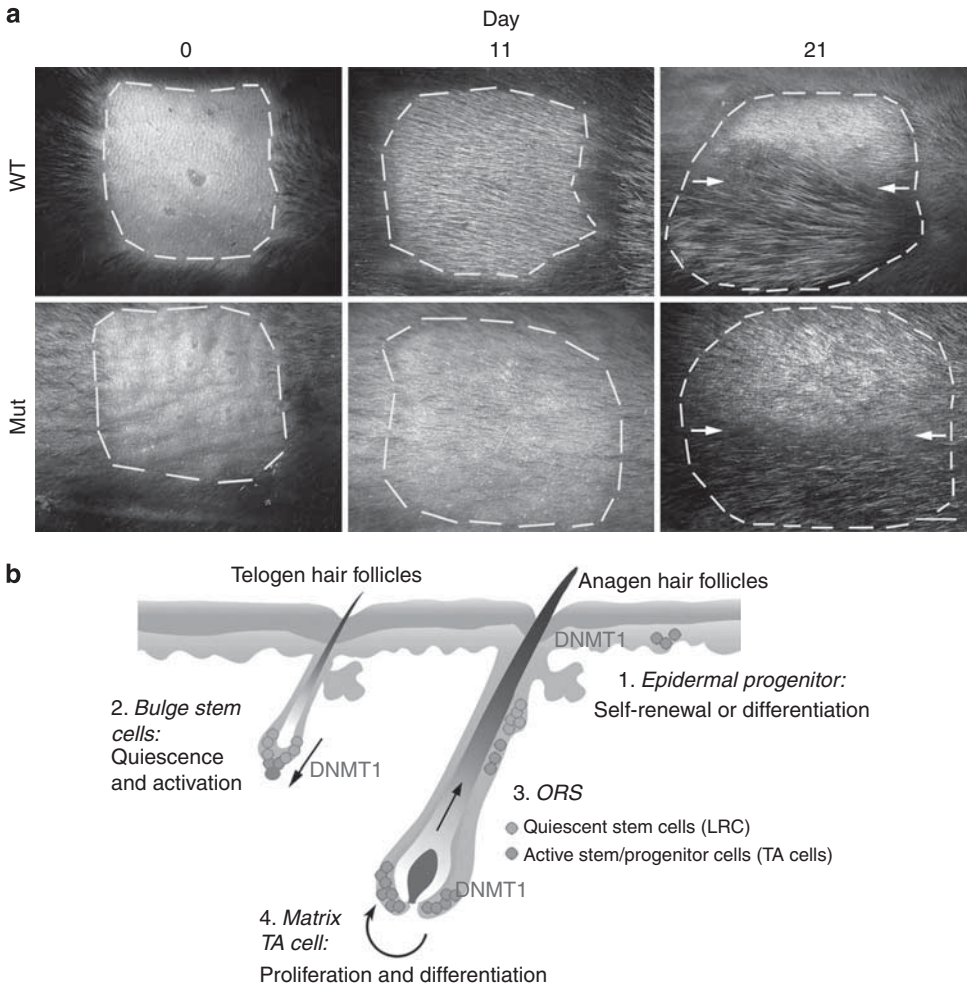

Figure 6. K14-Cre DNMT1$^{fl/fl}$ hair follicles show delay regeneration after plucking and summary diagram. (**a**) Hairs in a 1-cm^2 area are stripped with wax. At day 11 after waxing, new hairs appear in wild type (WT) but not in mutants (Mut). At day 21, both hairs have entered telogen. Upper half of the plucked region was shaved to see whether they are still in anagen (above green arrows). Bar = 2 mm. (**b**) Schematic summary showing the roles of DNA methyltransferase 1 (DNMT1) in skin morphogenesis. DNMT1 is involved in regulating epidermal progenitors and also hair follicle homeostasis. In the epidermis, mutant epidermis becomes thicker. In hair follicles, DNMT1 is involved in regulating the proliferation and apoptosis of bulge label-retaining cell (LRC) stem cells, outer root sheath (ORS), and matrix transient-amplifying (TA) cells. When DNMT1 is reduced, the probability of successful stem cell activation progressively decreases, leading to disrupted homeostasis in the epidermis, hair follicle cycling, and response to plucking. Reduction of hair fibers and follicles lead to the progressive alopecia phenotype. The color reproduction of this figure is available in the online version of the article.

DISCUSSION

Here we first discuss the epidermal and hair phenotype, and then the implications for DNMT activity on the homeostasis of stem, TA, and differentiated cells.

Epidermis phenotype

In the skin, DNMT1 is expressed in the basal layer of the epidermis. A recent study focused on its function in the human epidermis differentiation *in vitro* and found that DNMT1 was expressed in undifferentiated cells and is required for self-renewal of epidermal progenitor cells. The small hairpin RNA-mediated suppression of DNMT1 led to decreased capabilities of self-renewal and precocious epidermal differentiation (Sen *et al.*, 2010). Our *in vivo* study on mice with genetic changes is distinct from this published work. Interestingly, we observed that the thickness of mutant epidermis is uneven. Regions with thickened epidermis have increased proliferation compared with WT. This finding may imply a compensatory mechanism. In addition, differentiation markers such as involucrin appear patchy: expressed in the basal and suprabasal layer yet not in all suprabasal cells. Histone methyl transferase, EZH (enhancer of zeste), expression has been disrupted in the skin (Ezhkova *et al.*, 2011). EZH1- and EZH2-null hair follicles degenerate because of defective proliferation and increased apoptosis. Paradoxically, the mice also show hyperproliferation in the epidermis. Thus, the epidermis in our mutant can be thicker and individual cells appear larger, and this pathology becomes

more pronounced in the older mutants (Figures 2e and 4a). More work will be required to study the molecular differences.

Hair phenotype

Although the hair number appears normal in newborn mice, the number of hair fibers is progressively lost as mutant mice mature to adulthood. The number of hair fibers lost (>50%) is much greater than the reduction in hair follicles (20%), as many follicles stay in telogen in aging mice. Mutant mice show high variability in the size of hair follicles. Some follicles are smaller than normal, whereas some follicles are much larger (twice the diameter) with an enlarged hair canal (almost 5 times wider; Figure 4b). Although many molecules are suggested to regulate hair development, regeneration, and cycling (Botchkarev and Paus, 2003; Mikkola, 2007), few have been implicated in regulating hair size. Sharov *et al.* (2006) found that epithelial Noggin can modulate hair follicle size and hair fiber thickness. Hair size and diameter can be regulated by β-catenin expressed within the dermal papilla (Enshell-Seijffers *et al.*, 2010). The loss of uniform hair follicle size in our DNMT1-deleted mice implies that stem cell homeostasis is lost to varied degrees across the mouse skin. We speculate that it is possible that DNMT1 activity may be used to modulate hair follicle size in different body regions.

Hair fibers, which form on the mutant skin, do not show apparent architectural abnormalities or defective differentiation. All hair subtypes do exist. Unlike the uneven size of follicles, the hair fibers are consistently shorter in length and thinner in diameter.

Roles of DNMT1 in homoeostasis maintenance in hair follicles

Mutant hair follicles exhibit decreased TA cell proliferation in the ORS. They also demonstrate reduced upward migration. There is increased apoptosis in the hair matrix, ORS, and bulge area and increased DNA damage in the hair matrix. We found that γH2AX is increased significantly in the DNMT1-defective hair matrix cells. DNMT1-deficient HeLa and HCT116 cells attenuate the cellular response to DNA damage by 5-aza cytodine and block expression of γH2AX (Palii *et al.*, 2008). Accumulation of this damage in time may lead to degeneration and loss of hair follicles, and eventually the alopecia phenotype in aged mice.

However, K14 is expressed in the ORS, but not in the matrix. Whether the effect on hair matrix is directly mediated by DNMT or results from disrupted homeostasis of cell populations within the hair follicle remains to be studied. This line of research may be approached in the future by mating hair matrix–specific Cre with floxed DNMT1 mice to drive the expression of deleted DNMT1 to the matrix.

As mutant mouse hairs still undergo cycling and can respond to plucking, bulge stem cells can be activated. However, this ability gradually decreases as mice age, as evidenced by the increased telogen period in old mutants. The inability to activate stem cells for anagen reentry could be due to depletion of hair stem cells or over-quiescent stem cells that fail to respond to activation signals. We found that the mutant and WT bulge cells express approximately similar levels of K15, implying that the number of stem cells is not exhausted. Thus, with a defect in DNMT, hair bulge stem cells do seem to maintain a reasonable population size, and are capable of being activated to become hair germs and form hairs. However, the activation process takes longer and occurs with lesser efficiency, and the ability for self-renewal is also compromised. Thus, over time, the number of successfully formed hair filaments reduces and the some follicles degenerate. The detailed molecular mechanism in the DNMT-deficient bulge remains to be investigated. This is consistent with the idea that the activation of hair stem cells is a stochastic event (Plikus *et al.*, 2011); we think that the observed progressive alopecia phenotype is due to a decreasing probability of successful anagen reentry. Higher expression of P16 is consistent with this thought.

Progressive loss of DNMT1 protein or enzyme activity has been reported in aging human fibroblasts (Casillas *et al.*, 2003), suggesting that DNMT1 loss in the epithelium may be part of the aging process of the skin. Interestingly, K15-positive stem cells remaining in the bald scalp of patients with human androgenetic alopecia cannot be activated to become proliferative hair germs (Garza *et al.*, 2011). Future work will identify the molecular targets of DNMT in these stem cells and find out the relationship between mouse epidermal DNMT defects and human androgenetic alopecia.

MATERIALS AND METHODS

Generation and analysis of tissue-specific K14-Cre DNMT1$^{fl/fl}$ mice

Homozygous mice carrying the DNMT1$^{fl/fl}$ allele (Fan *et al.*, 2001; Jackson-Grusby *et al.*, 2001) were crossed with mice carrying the K14-Cre transgene (Andl *et al.*, 2004; Hosokawa *et al.*, 2009) and bred to homozygosity. Heterozygous mice did not show a phenotype. Cre excision resulted in an out-of-frame deletion of exons 4 and 5 producing a nonfunctional DNMT1 allele. The use of transgenic mice is approved by the USC Institutional Animal Care and Use Committee. Mice were genotyped according to Jackson-Grusby *et al* (2001). Briefly, genomic DNA was amplified by PCR. Primers for the DNMT1 5′ lox site, P1 (5′-GGGCCAGTTGTGT GACTTGG-3′) and P2 (5′-CTTGGGCCTGGATCTTGGGGA-3′), amplify a 334-bp WT and 368-bp DNMT1$^{fl/fl}$ fragment. Cre primers were Cre-F (5′-TTGCCCCTGTTTCACTATCCAG-3′) and Cre-R (5′-ATGGATTTCCGTCTCTGGTG-3′). Cre-recombination efficiency was assessed by PCR and western blot from genomic DNA and nuclear protein procured from the epithelium at multiple ages. Primers P1 and P2 amplified the floxed allele and P1 and P3 (5′-ATGCATAGGAACAGATGTGTGC-3′) amplified the recombinant allele. The deletion efficiency was determined as the ratios of the recombinant allele to floxed allele.

Measurement of hair number, length, and types

For hair number measurements, anagen-stage dorsal skin was fixed in 4% paraformaldehyde and dehydrated through an ethanol series and counted with skin inverted ($n=10$ mice). The type and length of each fiber was determined under a dissection microscope ($n=10$ mice).

Immunochemical procedure

Section IHC was performed on mouse dorsal skin samples following the procedure of Jiang *et al.* (1998). The following primary antibodies were used: rabbit anti-DNMT1 (1:200, Abcam, Cambridge, MA), mouse anti-K14 (1:200, Thermo Fisher Scientific, Fremont, CA), mouse anti-K10 (1:200, Thermo Fisher Scientific), mouse anti-AE13 (1:200, Abcam), mouse anti-AE15 (1:200, Santa Cruz Biotechnology, Santa Cruz, CA), mouse anti-involucrin (1:200, Thermo Fisher Scientific), rabbit antiphospho-H2AX (1:100; Cell Signaling Technology, Danvers, MA), rabbit anti-Lef1 (1:100, Cell Signaling Technology), rabbit anti-IAP (from Dr G Fan) (Hutnick *et al.*, 2010), rabbit anti-K15, and rabbit anti-Ki67 (1:500, Thermo Fisher Scientific). Western blotting was performed as described by Jiang *et al.*, 2011.

BrdU, CldU, and IdU labeling

For label-retaining cell labeling, neonatal mice were subcutaneously injected with CldU (50 mg per kg body weight) twice daily for 3 days ($n = 3$), from the third day after birth. After chasing for 8 weeks, dorsal skin tissues were excised. For the detection of proliferating cells, mice with hair follicles at anagen day 6 were given intraperitoneal injections of BrdU (100 mg BrdU per kg body weight; Sigma-Aldrich, St Louis, MO) and killed 1 hour after injection. Alternatively, mice were given CldU (100 mg CldU per kg body weight; Sigma-Aldrich) for 11.5 hours and IdU for 0.5 hours, and then killed. Tissues were fixed and sectioned as described above and stained with mouse anti-BrdU (Millipore, Temecula, CA, MAB3424), rat anti-CldU (Abcam, Ab6326-250), and mouse anti-IdU (BD, 347580) antibodies. Secondary antibody was conjugated with Alexa Fluor 594 (Invitrogen, Carlsbad, CA).

TUNEL assay

In situ cell death detection kit (Roche, Pleasanton, CA) was used.

Hair plucking and regeneration

We plucked pelage hairs from a 1-cm^2 area of the 6-month-old mice with wax. Pictures were taken every 2 days until the hair coat regenerated.

CONFLICT OF INTEREST

The authors state no conflict of interest.

ACKNOWLEDGMENTS

This research was supported by the NIAMS through grants AR 42177, 47364 (to C-MC), 60306 (to C-MC and T-XJ), and NS051411 (to GF). JL is supported by the National Natural Science Foundation of China. We thank Dr Chi-Chiang Chen and Dr Sung-Jan Lin for help and discussion, and Dr Juehua Yu for performing IAP immunostaining. Confocal microscopy was performed by the Cell and Tissue Imaging Core of the USC Research Center for Liver Diseases, NIH grant P30 DK048522.

REFERENCES

Andl T, Ahn K, Kairo A *et al.* (2004) Epithelial Bmpr1a regulates differentiation and proliferation in postnatal hair follicles and is essential for tooth development. *Development* 131:2257–68

Blanpain C, Fuchs E (2009) Epidermal homeostasis: a balancing act of stem cells in the skin. *Nat Rev Mol Cell Biol* 10:207–17

Botchkarev VA, Paus R (2003) Molecular biology of hair morphogenesis: development and cycling. *J Exp Zool B Mol Dev Evol* 298:164–80

Casillas MA Jr, Lopatina N, Andrews LG *et al.* (2003) Transcriptional control of the DNA methyltransferases is altered in aging and neoplastically-transformed human fibroblasts. *Mol Cell Biochem* 252:33–43

Cotsarelis G (2006) Epithelial stem cells: a folliculocentric view. *J Invest Dermatol* 126:1459–68

Enshell-Seijffers D, Lindon C, Kashiwagi M *et al.* (2010) beta-catenin activity in the dermal papilla regulates morphogenesis and regeneration of hair. *Dev Cell* 18:633–42

Ezhkova E, Lien WH, Stokes N *et al.* (2011) EZH1 and EZH2 cogovern histone H3K27 trimethylation and are essential for hair follicle homeostasis and wound repair. *Genes Dev* 25:485–98

Fan G, Beard C, Chen RZ *et al.* (2001) DNA hypomethylation perturbs the function and survival of CNS neurons in postnatal animals. *J Neurosci* 21:788–97

Garza LA, Yang CC, Zhao T *et al.* (2011) Bald scalp in men with androgenetic alopecia retains hair follicle stem cells but lacks CD200-rich and CD34-positive hair follicle progenitor cells. *J Clin Invest* 121:613–22

Goldberg AD, Allis CD, Bernstein E (2007) Epigenetics: a landscape takes shape. *Cell* 128:635–8

Hosokawa R, Deng X, Takamori K *et al.* (2009) Epithelialspecific requirement of FGFR2 signaling during tooth and palate development. *J Exp Zool B Mol Dev Evol* 312B:343–50

Hutnick LK, Huang X, Loo TC *et al.* (2010) Repression of retrotransposal elements in mouse embryonic stem cells is primarily mediated by a DNA methylation-independent mechanism. *J Biol Chem* 285:21082–91

Jackson-Grusby L, Beard C, Possemato R *et al.* (2001) Loss of genomic methylation causes p53-dependent apoptosis and epigenetic deregulation. *Nat Genet* 27:31–9

Jiang TX, Stott NS, Widelitz RB *et al.* (1998) Current methods in the study of avian skin appendages. In: (Chuong CM, ed). *Molecular Basis of Epithelial Appendage Morphogenesis*. Landes: Austin, TX, 359–408

Jiang TX, Tuan TL, Wu P *et al.* (2011) From buds to follicles: matrix metalloproteinases in developmental tissue remodeling during feather morphogenesis. *Differentiation* 81:307–14

Lynch MH, O'Guin WM, Hardy C *et al.* (1986) Acidic and basic hair/nail (''hard'') keratins: their colocalization in upper cortical and cuticle cells of the human hair follicle and their relationship to ''soft'' keratins. *J Cell Biol* 103:2593–606

Mikkola ML (2007) Genetic basis of skin appendage development. *Semin Cell Dev Biol* 18:225–36

Mortusewicz O, Schermelleh L, Walter J *et al.* (2005) Recruitment of DNA methyltransferase I to DNA repair sites. *Proc Natl Acad Sci USA* 102:8905–9

Palii SS, Van Emburgh BO, Sankpal UT *et al.* (2008) DNA methylation inhibitor 5-Aza-2′-deoxycytidine induces reversible genome-wide DNA damage that is distinctly influenced by DNA methyltransferases 1 and 3B. *Mol Cell Biol* 28:752–71

Peters EM, Tobin DJ, Botchkareva N *et al.* (2002) Migration of melanoblasts into the developing murine hair follicle is accompanied by transient c-Kit expression. *J Histochem Cytochem* 50:751–66

Plikus MV, Baker RE, Chen CC *et al.* (2011) Self-organizing and stochastic behaviors during the regeneration of hair stem cells. *Science* 332:586–9

Plikus MV, Chuong CM (2008a) Complex hair cycle domain patterns and regenerative hair waves in living rodents. *J Invest Dermatol* 128:1071–80

Plikus MV, Mayer JA, de la Cruz D *et al.* (2008b) Cyclic dermal BMP signalling regulates stem cell activation during hair regeneration. *Nature* 451:340–4

Schmidt-Ullrich R, Paus R (2005) Molecular principles of hair follicle induction and morphogenesis. *Bioessays* 27:247–61

Sen GL, Reuter JA, Webster DE *et al.* (2010) DNMT1 maintains progenitor function in self-renewing somatic tissue. *Nature* 463:563–7

Sharov AA, Sharova TY, Mardaryev AN *et al.* (2006) Bone morphogenetic protein signaling regulates the size of hair follicles and modulates the expression of cell cycle-associated genes. *Proc Natl Acad Sci USA* 103:18166–71

Stenn KS, Paus R (2001) Controls of hair follicle cycling. *Physiol Rev* 81:449–94

Zhang YV, Cheong J, Ciapurin N *et al.* (2009) Distinct self-renewal and differentiation phases in the niche of infrequently dividing hair follicle stem cells. *Cell Stem Cell* 5:267–78